acta physica slovaca vol. 56 No. 4, 503 – 509 **August 2006**

DILEPTON PRODUCTION FROM HYDRODYNAMICALLY EXPANDING FIREBALL

V. V. Skokov[1,a,b], **V. D. Toneev**[,a,b]
[a] *Bogoliubov Laboratory of Theoretical Physics, Joint Institute for Nuclear Research, 141980, Dubna, Russia*
[b] *Gesellschaft für Schwerionenforschung, 64291 Darmstadt, Germany*

Received 5 December 2005, in final form 7 February 2006, accepted 9 February 2006

A hybrid model is put forward for describing relativistic heavy ion collisions. The early interaction stage responsible for entropy creation is calculated within the transport Quark-Gluon String Model resulting in an initial state. The passage to subsequent isoentropic expansion proceeds with exact account for all conservation laws. Relativistic 3D hydrodynamics with the mixed phase equation of state is applied to this expansion stage. Essential differences in evolution of a fireball, described within this model and one for the Bjorken regime, are noted. The in-medium modified e^+e^- spectra are studied and confronted with the recent CERES/NA45 data for 8% central Pb+Au collisions at the bombarding energy 158 AGeV.

PACS: 25.75.-q 24.10.Nz 24.10.Pa

Electromagnetic probes and, in particular, di-electrons play an exceptional role providing almost undisturbed information on a state of highly compressed and hot nuclear matter (fireball) formed in relativistic heavy ion collisions. Generally, dilepton yield depends on both global properties of matter constituents (hadrons and/or quarks, gluons) defined by the equation of state and also on individual constituent properties related to their in-medium modification. Such a modification has been observed by the CERES Collaboration in the analysis of the e^+e^- invariant mass spectra from central Pb+Au collisions [1]. The measured dilepton excess in the range of invariant dilepton masses $0.2 \lesssim M \lesssim 0.7$ GeV may be interpreted in terms of a strong in-medium ρ-meson modification (see review articles [2, 3]). Many papers are devoted to the analysis of these CERES data but mainly two scenarios of hadron modification are available on the market: Consideration based on the Brown-Rho scaling hypothesis [4] assuming a dropping ρ mass and that for a strong broadening as found in the many-body approach by Rapp and Wambach [3, 5]. Unfortunately, a very simplified dynamical treatment is usually applied which obscures the origin of the model agreement or disagreement with experiment.

In this paper, we make emphasis on nuclear interaction dynamics to clarify which states in the main contribute to the observed dilepton yield as well as which are the model parameters used. We confront our model calculations with the recent CERES/NA45 results for 8% central Pb+Au collisions at the bombarding energy 158 AGeV [6].

We treat dynamics of heavy ion collisions in terms of a hybrid model where the initial interaction stage is described by the transport Quark Gluon String Model (QGSM) [7].

[1] E-mail address: vvskokov@theor.jinr.ru

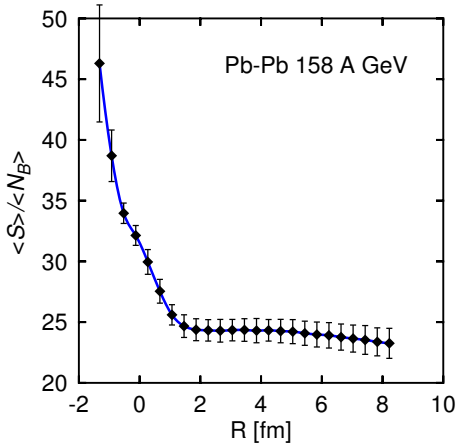

Fig. 1. Average entropy S per average baryon charge Q_B for participants versus relative distance between the centers of two colliding Pb nuclei at E_{lab} =158 AGeV.

In Fig. 1, the temporal dependence of the ratio of entropy S to the total participant baryon charge Q_B is shown for Pb+Pb collisions at the impact parameter $b = 2.5$ fm and bombarding energy 158 AGeV evaluated within QGSM. Being calculated on a large 3D grid, this ratio is less sensitive to particle fluctuation as compared to entropy itself. Small values of Q_B at the very beginning of interaction result in large values of the S/Q_B ratio. It is clearly seen that this ratio is practically kept constant for $R \gtrsim 1.5$ fm, i.e., a little bit later on the moment when two nuclei completely overlap ($R = 0$). The stage for $R \gtrsim 1.5$ fm may be treated as isoentropic expansion.

So the subsequent stage starts from $R \approx 1.5$ fm, which corresponds to the kinetic evolution time moment $t_{kin} = 1.8$ fm/c and evolves further as a isoentropic expansion. This stage is described within the relativistic 3D hydrodynamics. A full set of hydrodynamic equations is solved numerically by the FCT-SHASTA method [8] with the mixed phase Equation of State (EoS) [9]. This thermodynamically consistent EoS uses the modified Zimanyi mean-field interaction for hadrons [10, 11] which reproduces properties of the saturated nuclear matter at the normal density $n_B = n_0$ and is in good agreement with the Danielewicz constraints to EoS [12] (see Fig. 2). This mixed phase EoS also includes the interaction between hadron and quark-gluon phases, which results in a cross-over deconfinement phase transition. In addition to the model prescription in Ref. [9], the hard thermal loop term was self-consistently added to the interaction of quarks and gluons to get the correct asymptotics at $T >> T_c$ and to provide reasonable agreement between the model results and lattice QCD calculations at finite temperature T and chemical potential μ_B [13].

To proceed from kinetics to hydrodynamics keeping exactly the conservation laws, we evaluate locally on the 3D grid the energy-momentum tensor, baryon density and velocity profile at the time moment $t_{kin} = 1.8$ fm/c and then treat these quantities as an initial (t=0) state of a fireball for its subsequent 3D hydrodynamic evolution. The temporal dependence of the average

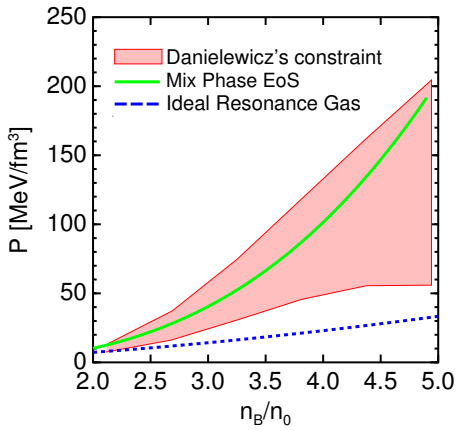

Fig. 2. Baryon density dependence of pressure at the zero temperature. The mixed phase model results are plotted by the solid line, the dashed one corresponds to the ideal gas EoS. The shaded area is the constraint obtained by Danielewicz *et al.* [12].

energy density is presented in Fig. 3 for the expansion stage. The average quantity is defined as

$$\bar{\varepsilon}(t) \equiv \bar{\varepsilon} = \int d^3x\, \varepsilon(t,x)\, w(t,x) \;/\; \int d^3x\, w(t,x), \tag{1}$$

where $w(t,x)$ is its time-space distribution.

As is seen, the initial energy density is quite high, $\bar{\varepsilon}(t \approx 0) \sim 5.5\, GeV/fm^3$. The appropriate compression ratio $\bar{n}_B(0)/n_0$ reaches about 4.2. Note that these values characterize the initial locally equilibrium state of the fireball and are noticeably lower than the peak-values estimated in nonequilibrium models with averaging over some limited spacial volume [15]. Average energy density falls down in time and its behavior at the SPS energy remarkably differs from that for the Lorentz invariant Bjorken expansion regime (see the dashed line in Fig. 3). The scaled Bjorken solution of 1D hydrodynamics [14] is not applicable to the first moments of hydrodynamic expansion and more corresponds to the asymptotic expansion regime. However, if the same initial energy density is assumed for the Bjorken expansion, one can see that the fireball life time becomes very short. In addition, this simple solution does not reproduce some flattening of the time dependence of the energy density observed for $t \gtrsim 8$ fm/c. The origin of this effect is demonstrated in the right side of Fig. 3.

In our consideration, the hydrodynamic evolution of a cell ends at the freeze-out defined by the condition that the local energy density (including 6 neighbor cells) is below a certain value $\varepsilon_i < \varepsilon_{fr} = 0.3$ GeV/fm^3. This condition may be fulfilled locally at the periphery of the expanding system from the very beginning of expansion and works continuously during the whole evolution. The frozen cell will not participate in a further dynamical process but contribute to the "hadron decay cocktail". The system volume V presented in Fig. 3 is defined as the sum over all cells with nonvanishing energy density ε_i besides frozen cells. As is seen, the system volume naturally starts to grow with expansion but later on the competition between expansion

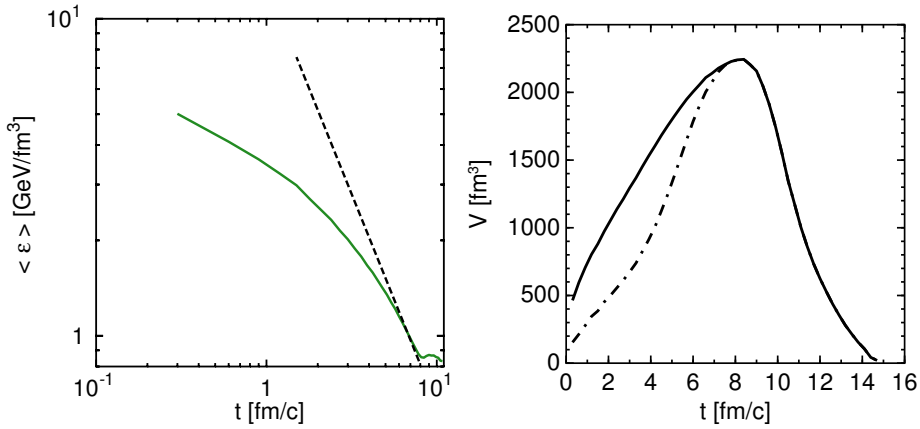

Fig. 3. The average energy density (the left panel) and volume (the right panel) of the expanding fireball formed in central Pb+Pb collisions. The dotted line (in arbitrary normalization) shows the Bjorken solution [14] for 1D expansion with the ultrarelativistic ideal gas EoS and the dot-dashed line corresponds to the account for hadronic phase cells only (see the text).

and freeze-out effect is getting stronger and so V drops for $t \gtrsim 8$ fm/c. Certainly, this effect is absent in the Bjorken regime. According to the mixed phase model [9], in every state generally there is a homogeneous mixture of free quarks/gluons and bound quarks (hadrons) with quark densities ρ^{Q+G}_{quarks} and ρ^{H}_{quark}, respectively. One may conditionally define the hadronic phase as $\rho^{H}_{quark} > \rho^{Q+G}_{quarks}$. As follows from Fig. 3 (the dot-dashed line), the admixture of the quark/gluon phase is negligible for the expansion time $t \gtrsim 4$ fm/c which roughly corresponds to the average temperature of the system $\bar{T}(t \approx 4) \approx 180$ MeV.

The full set of the freeze-out cells or the time-space freeze-out surface, where hadrons are decoupled, defines all characteristics of observable hadrons. To transform these frozen cells into hadrons, we use the procedure described in [16]. The freeze-out parameter ε_{fr} is controlled by the pion yield at high colliding energies (but weakly sensitive at moderate energies, similarly to [16]). Having in mind that the main emphasis will be made on the $\pi\pi$ channel, in Fig. 4 the rapidity and transverse mass spectra of observed pions are shown for central Pb+Pb collisions at the top SPS energy. The agreement between model calculations and data of the NA49 experiment is quite reasonable.

To find observable invariant mass spectra of dileptons, one should integrate the emission rate $d^8N_{ee}(T(x), \mu_B(x), M, \eta, q_T)/dt\, d^3x\, d^4q$ over the whole time-space evolution $\int dt d^3x$ and add the contribution from the freeze-out surface (hadron cocktail). If we are interested in the e^+e^- invariant mass M distributions in some pseudo-rapidity window $\Delta\eta_{e\pm}$ (like in the CERES experiment) and treat the fireball evolution on average, then in this case

$$\frac{d^2N_{ee}}{dMd\eta} = \frac{M}{\Delta\eta_{e_\pm}} \int d\eta \int V(t)dt \int_0^{2\pi} d\phi \int_0^{\infty} q_T dq_T \frac{d^5N_{ee}(\bar{T}(t), \bar{\mu}_B(t), M, \eta, q_T)}{dtd^4q} Acc, \quad (2)$$

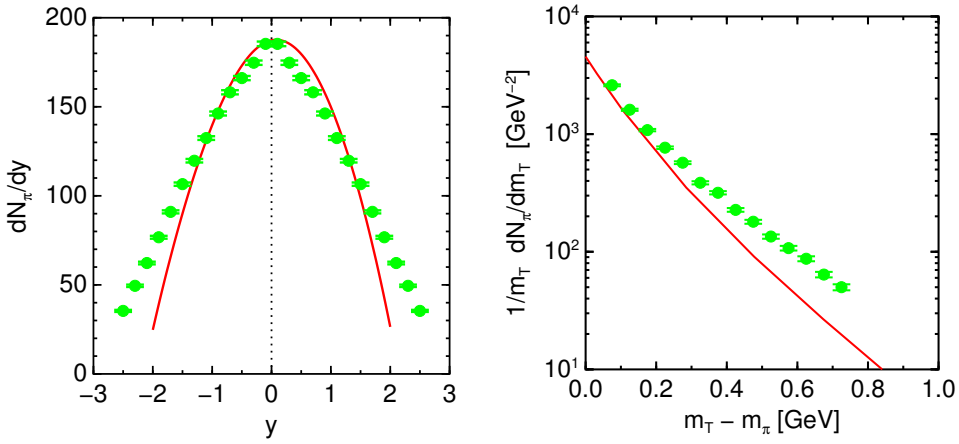

Fig. 4. Rapidity (the left panel) and transverse mass (the right panel) distributions of π^- meson from central Pb+Pb collision at $E_{lab} = 158$ AGeV. Experimental points are taken from [17].

where the factor $Acc \equiv Acc(M, \eta, q_T)$ takes into account the experimental acceptance.

To simplify more our task, we consider only the main emission channel $\pi\pi \to l^+l^-$. The dilepton emission rate is [18]

$$\frac{d^5N}{dtd^4q} = -\mathcal{L}(M)\,\frac{\alpha^2}{\pi^3 q^2}\,f_B(q_0,\bar{T})\,\mathrm{Im}\Pi_{em}(q,\bar{T},\bar{\mu}_b), \tag{3}$$

where the Bose distribution function is defined as $f_B(q_0,T) = (e^{q_0/\bar{T}} - 1)^{-1}$, the 4-momentum transfer $q^2 = M^2 = q_0^2 - \mathbf{q}^2$ and the lepton kinematic factor is

$$\mathcal{L}(M) = \left(1 + 2\frac{m_l^2}{M^2}\right)\sqrt{1 - 4\frac{m_l^2}{M^2}} \tag{4}$$

with the lepton mass m_l.

We will consider electro-magnetic current correlation function $\Pi_{em}(q,\bar{T},\bar{\mu}_b)$ in two different scenarios: (I) the finite temperature modification of pion gas properties [18]; (II) droping mass scenario [3].

Dilepton invariant mass spectra from 8% centrality Pb+Pb collisions at $E_{lab} = 158$ AGeV are presented in Fig. 5. Experimental acceptance is taken into account for both hadron cocktail and $\pi\pi$ annihilation channel. This channel is calculated on the absolute basis without any fitting parameters. As one can see, the 1st scenario slightly overestimates the dilepton yield near the ρ meson mass and underestimates it in the $0.3 \lesssim M \lesssim 0.6$ range though these values are essentially above the hadron cocktail data. This overestimation is explained mainly by simplified dynamics of dilepton production, using average evolution trajectories and rough approximations for proceeding to hadronic phase. The depleted yield of low-mass dileptons results from neglecting "sobar" contribution (nucleonic loops) into the emission rate.

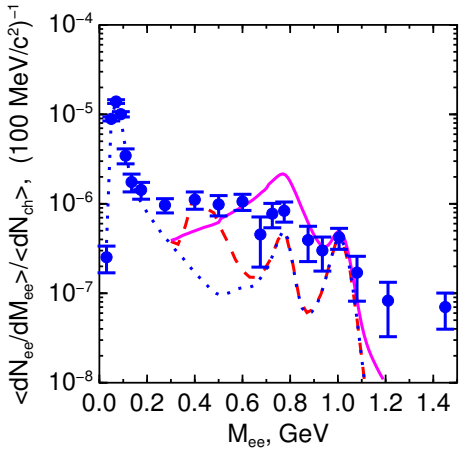

Fig. 5. Invariant mass distribution of dileptons from 8% central Pb+Pb collisions at the beam energy 158 AGeV. Experimental points are from [6]. The solid and dashed curves are calculated using the finite temperature modification in pion gas and the ρ dropping mass scenario (5), respectively. The dotted line indicates an estimate of "hadron decay cocktail".

To simulate droping mass scenario, we modify the in-medium mass of ρ-meson as commonly employed in the literature :

$$m_\rho^* = m_\rho(1 - 0.18 \cdot \bar{n}_B(t)/n_0)\left(1 - [\bar{T}(t)/T_c]^2\right)^{0.3} \tag{5}$$

and simultaneously apply the same modification to the vector dominance coupling $m_\rho^2/g \to m_\rho^{*2}/g^*$. The first factor in Eq. (5) was estimated by Hatsuda and Lee [20] according to the QCD sum rules. The temperature dependence in Eq. (5) is motivated by the T-dependence of the quark condensate.

The results for the dropping ρ mass scenario are also plotted in Fig. 5. In this case, the low dilepton mass region $0.2 \lesssim M \lesssim 0.7$ is also populated but the free ρ mass region is essentially underestimated. The shape of the M-distributions in these two scenarios is quite different. The simplified dynamical assumptions mentioned above also influence the ρ mass scaling results. However, the large shift of the e^+e^- invariant mass spectrum towards low M is mostly due to using the T-dependent factor in Eq. (5), which seems to be not very justified [21].

Finally, inclusion of the full dynamics of heavy ion collisions in evaluation of dilepton production is quite important. Comparison of evolution within the proposed dynamical model with the popular Bjorken regime shows essential differences which may manifest themselves in dilepton observables. Full dynamical calculations allow one to probe not only the shape of the e^+e^- spectra from $\pi\pi$ annihilation but also to estimate the absolute contribution of this channel. Certainly, the simplifying dynamical assumptions used should be overcome as well as other dilepton production channels should be added, in particular those coming from a quark phase. In this respect, it is of interest to note that the mixed phase EoS, in principle, opens new possible channels due to interaction between hadron and quark/gluon phases. The hadron decay cocktail should

also be calculated within the same model. This work is now in progress.

Acknowledgement: We are grateful to Yu.B. Ivanov and V.N. Russkih for numerous discussions concerning hydrodynamic code and freeze-out procedure. We thank S. Yurevich for providing us with the hadronic cocktail data for the CERES/NA45 experiment. One of us (VS) thanks organizers of the QM2005 conference for making his participation possible. This work was supported in part by DFG (project 436 RUS 113/558/0-3) and RFBR (grant 06-02-04001).

References

[1] G. Agakishiev *et al.*, CERES Collaboration: *Phys. Rev. Lett.* **75** (1995) 1272; G. Agakishiev *et al.*, CERES Collaboration: *Phys. Lett. B* **422** (1998) 405 [arXiv:nucl-ex/9712008]; D. Adamova *et al.*, CERES/NA45 Collaboration: *Phys. Rev. Lett.* **91** (2003) 042301 [arXiv:nucl-ex/0209024]

[2] W. Cassing, E. L. Bratkovskaya: *Phys. Rep.* **308** (1999) 65

[3] R. Rapp, J. Wambach: *Adv. Nucl. Phys.* **25** (2000) 1

[4] G. E. Brown, M. Rho: *Phys. Rev Lett.* **66** (1991) 2720

[5] R. Rapp, G. Chanfray, J. Wambach: *Phys. Rev. Lett.* **76** (1996) 368 [arXiv:hep-ph/9508353]

[6] CERES/NA45 Collaboration: *J. Phys. G* **30** (2004) S1007; *J. Phys. G* **30** (2004) S2027; S. Yurevich (privite communication)

[7] N. S. Amelin, K. K. Gudima, S. Y. Sivoklokov, V. D. Toneev: *Sov. J. Nucl. Phys.* **52** (1990) 172 [*Yad. Fiz.* **52** (1990) 272]; N. S. Amelin, E. F. Staubo, L. P. Csernai, V. D. Toneev, K. K. Gudima: *Phys. Rev. C* **44** (1991) 1541; V. D. Toneev, N. S. Amelin, K. K. Gudima, S. Yu. Sivoklokov: *Nucl. Phys. A* **519** (1990) 463c

[8] V. V. Skokov, V. D. Toneev: JINR Preprint P2-2005-95 (2005) [accepted for *Yad. Fiz.*]

[9] V. D. Toneev, E. G. Nikonov, B. Friman, W. Nörenberg, K. Redlich: *Eur. Phys. J. C* **32** (2004) 399 [arXiv:hep-ph/0308088]

[10] J. Zimanyi, B. Lukacs, P. Levai, J. P. Bondorf and N. L. Balazs, Nucl. Phys. A **484** (1988) 647

[11] E. G. Nikonov, V. D. Toneev and A. A. Shanenko, Phys. Atom. Nucl. **62** (1999) 1226 [Yad. Fiz. **62** (1999) 1301]

[12] P. Danielewicz, R. Lacey, V.G. Lynch: *Science* **298** (2002) 1592 [arXiv:nucl-th/0208016]

[13] Z. Fodor: *Nucl. Phys. A* **715** (2003) 319; F. Csikor, G. I. Egri, Z. Fodor, S. D. Katz, K. K. Szabo A. I. Toth, *JHEP* **405** (2004) 46

[14] J. P. Bjorken: *Phys. Rev. D* **27** (1984) 140

[15] B. Friman, W. Nörenberg, V. D. Toneev: *Eur. Phys. J. A* **3** (1998) 165 [arXiv:nucl-th/9711065]; Bao-An Li, C. M. Ko: *Phys. Rev. C* **52** (1995) 2037

[16] Yu. B. Ivanov, V. N. Russkikh, V. D. Toneev: arXiv:nucl-th/0503088

[17] S. V. Afanasiev *et al.*, NA49 Collaboration: *Phys. Rev. C* **66** (2002) 054902 [arXiv:nucl-exp/0205002]

[18] C. Gale, J.I. Kapusta: *Nucl. Phys. B* **357** (1991) 65

[19] F. Klingl, N. Kaiser, W. Weise: *Z. Phys. A* **356** (1996) 193 [arXiv:hep-ph/9607431]

[20] T. Hatsuda, S. H. Lee: *Phys. Rev. C* **46** (1992) R34

[21] G. E. Brown, M. Rho: *Phys. Rept.* **396** (2004) 1